

A Study on Three Factors Influencing Uptake Rates of Nitric Acid onto Dust Particles

Chul Han Song* and Chung Man Kim¹⁾

Department of Environmental Science and Engineering, Gwangju Institute of Science and Technology (GIST),
1 Oryong-dong, Buk-gu, Gwangju 500-712, Korea

¹⁾Korea Ocean Research & Development Institute (KORDI), 104 Sinseong-ro, Yuseong-gu, Daejeon 305-343, Korea

*Corresponding author. Tel: +82-62-715-3276, E-mail: chsong@gist.ac.kr

ABSTRACT

Recent studies have indicated that the observed nitric acid (HNO_3) uptake rates (R_{HNO_3}) onto dust particles are much slower than R_{HNO_3} used in the previous modeling studies. Three factors that possibly affect R_{HNO_3} onto dust particles are discussed in this study: (1) the magnitude of reaction probability of HNO_3 (γ_{HNO_3}), (2) aerosol surface areas, and (3) gas-phase HNO_3 mixing ratio. Through the discussion presented here, it is shown that the use of accurate γ_{HNO_3} is of primary importance. We suggest that the use of γ_{HNO_3} values between $\sim 10^{-3}$ and $\sim 10^{-5}$ produces more realistic results than the use of γ_{HNO_3} values between $\sim 10^{-1}$ and $\sim 10^{-2}$ does, more accurately modeling the nitrate formation characteristics on/in dust particles. We also discuss two different types of aerosol surface area, active and geometric, since the use of different aerosol surface areas often leads to an erroneous result in R_{HNO_3} . In addition, the levels of the gas-phase HNO_3 are investigated with the example cases of TRACE-P DC-8 flights in East Asia. The HNO_3 levels were found to be relatively high, indicating that they can not limit nitrate formation in dust particles.

Key words: Reaction probability, Dust particles, Nitric acid, Uptake rates, Aerosol surface area

1. INTRODUCTION

Recently, several studies have reported that although East Asian dust particles have sufficient chemical aging (or contacting) times (say, 1-4 days) with atmospheric air pollutants, they were found to contain only small amounts of nitrate (and/or sulfate) (Song *et al.*, 2007; Song *et al.*, 2005; Maxwell-Meier *et al.*, 2004). This fact possibly indicates that the gas-to-particle nitric acid (HNO_3) uptake rates (R_{HNO_3}) onto dust particles are slower than previously estimated. This could also be an important correction to the results from pre-

vious studies (Meskhidze *et al.*, 2003; Song and Carmichael, 2001; Zhang and Carmichael, 1999; Dentener *et al.*, 1996). For example, Meskhidze *et al.* (2003) inferred from the data of TRACE-P DC-8 Flight #13 that total nitrate ($=\text{HNO}_3(\text{g})+\text{NO}_3^-(\text{p})$) distribution between gas phase and East Asian dust particles reaches a near equilibrium (refer to Fig. 4 in Meskhidze *et al.* (2003)). Their work supported the opposite idea that dust particles could contain a quite large amount of nitrate that could completely neutralize dust-originated cationic components such as Ca^{2+} and Mg^{2+} . This study, therefore, intends to discuss possible causes of this discrepancy in order to offer a convincing explanation.

Closely connected with this issue, controversy has continued regarding the magnitude of reaction probability of HNO_3 (γ_{HNO_3}) onto dust particles. Several research groups measured γ_{HNO_3} onto various types of dust particle, from proxy species of dust particles (e.g., $\alpha\text{-Al}_2\text{O}_3$, SiO_2 , CaCO_3 etc) to authentic Saharan and Gobi dust. However, a large difference in the magnitude of γ_{HNO_3} onto dust particles has been reported (Johnson *et al.*, 2005; Umann *et al.*, 2005; Harnisch and Crowley, 2001a, b; Underwood *et al.*, 2001a, b; Fenter *et al.*, 1995), as presented in Table 1. Here, the first group of γ_{HNO_3} has an order of magnitude from $\sim 10^{-1}$ to $\sim 10^{-2}$ (Umann *et al.*, 2005; Harnisch and Crowley, 2001a, b; Fenter *et al.*, 1995), compared to a range from $\sim 10^{-3}$ to $\sim 10^{-5}$ for the second group (Johnson *et al.*, 2005; Underwood *et al.*, 2001a, b).

The ultimate purpose of estimating (or measuring) γ_{HNO_3} is to apply the result to the chemistry-transport modeling studies. However, because of the large differences in the magnitude of γ_{HNO_3} onto dust particles, atmospheric modelers have been confused about which value should be adopted in their modeling studies (Song *et al.*, 2007; Bauer *et al.*, 2004; Zhang and Carmichael, 1999; Dentener *et al.*, 1996; and also the third group of γ_{HNO_3} as presented in Table 1). In addition, it appears that the parameterizations (or estimation method for γ_{HNO_3}) for describing the heterogeneous interac-

Table 1. Reaction Probability of HNO₃ onto dust particles.

γ_{HNO_3}	Type of Dust	Method	Reference
7.1×10^{-2}	Marble powder	Low pressure-flow reactor (Knudsen cell)	Fenter <i>et al.</i> (1995)
7.1×10^{-2}	CaCO ₃		
7.6×10^{-2}	Na ₂ CO ₃	Knudsen cell reactor	Harnisch and Crowley (2001a)
$1.5 (\pm 0.3) \times 10^{-1}$	CaCO ₃ (humid)		
6.0×10^{-2}	CaCO ₃ (dried)		
13.6×10^{-2}	Saharan Dust		
$17.1 (\pm 3) \times 10^{-2}$	Chinese Dust		
$14.0 (\pm 1.5) \times 10^{-2}$	Dolomite	Knudsen cell reactor	Harnisch and Crowley (2001b)
$11 (\pm 3) \times 10^{-2}$	Saharan Dust		
$6 (\pm 1.5) \times 10^{-2}$	Arizona Dust		
$10 (\pm 2.5) \times 10^{-2}$	CaCO ₃ (heated)		
$18 (\pm 4.5) \times 10^{-2}$	CaCO ₃ (unheated)		
$13 (\pm 3.3) \times 10^{-2}$	Al ₂ O ₃	Field study	Umann <i>et al.</i> (2005)
3.3×10^{-2} ¹⁾	Saharan Dust		
$5.2 (\pm 0.3) \times 10^{-5}$	Gobi Dust	Knudsen cell reactor	Underwood <i>et al.</i> (2001a)
$2.0 (\pm 0.1) \times 10^{-5}$	Saharan Dust		
1.4×10^{-3}	MgO (wet condition)	Knudsen cell reactor	Underwood <i>et al.</i> (2001b)
1.6×10^{-2}	CaO (wet condition)		
$2 \times 10^{-5} \times R_G$ ²⁾	Saharan Dust	Knudsen cell reactor	Johnson <i>et al.</i> (2005)
1.1×10^{-3}	China Loess		
$7 (\pm 4) \times 10^{-4}$	Dolomite		
$1.5 (\pm 0.4) \times 10^{-3}$	CaCO ₃		
0.1	Dust	Modeling study	Dentener <i>et al.</i> (1996)
0.01	Dust	Modeling study	Zhang and Carmichael (1999)
0.1	Dust	Modeling study	Bauer <i>et al.</i> (2004)
10^{-3} - 10^{-5} ³⁾	Dust	—	This study

Note: ¹⁾Values of 0.017-0.054 were reported; ²⁾Surface roughness factor; ³⁾Values recommended by this study.

tion between HNO₃ and dust particles are questionable. Therefore, an impartial discussion is urgently required about both the magnitudes of γ_{HNO_3} onto dust particles and the parameterizations for the heterogeneous interactions between HNO₃ and dust particles. In this study, we discuss all the relevant and yet contentious issues regarding the heterogeneous processes between gas-phase HNO₃ and dust particles. In addition, through this study we wish to provide a modeler's perspective regarding the chemical evolution of dust particles and the magnitude of γ_{HNO_3} onto dust particles.

2. DISCUSSION

2.1 Research and Theoretical Background

The HNO₃ uptake into dust particles causes the replacement of carbonate (CO₃²⁻) originally associated with crustal Ca²⁺ (and/or Mg²⁺) in dust particles via the following reaction:



Similar carbonate replacement reactions occur with the uptake of other acidic substances such as H₂SO₄ and SO₂. Based on this mechanism, Table 2 presents

the “dust chemical aging index”, defined as the ratio of estimated CO₃²⁻ equivalence ([CO₃²⁻] in $\mu\text{eq}/\text{m}^3$) to crustal cation equivalence ([Ca²⁺] + [Mg²⁺]) at several different locations in East Asia (Song *et al.*, 2007; 2005). As presented in Table 2, the ratios range from 0.39 to 0.87, indicating that the remaining carbonate fractions in the dust particles range from 39-87%, respectively, even after the chemical aging times of 24-84 hrs. Several single particle chemical analysis studies with East Asian dust particles reached the same conclusions (Ro *et al.*, 2005; Zhang *et al.*, 2003; Zhang and Iwasaka, 1999). The replaced CO₃²⁻ fractions of 13-61% are believed to be released from dust particles by nitrate (and/or sulfate) formation. The small percentages of the replaced carbonate, even with the long chemical aging times, are obvious evidences of slow R_{HNO_3} onto dust particles.

Assuming pseudo first-order kinetics (eqn. 1), R_{HNO_3} can be calculated by eqns. (1) and (2). In the equations, the magnitude of R_{HNO_3} can be affected by three factors: i) γ_{HNO_3} ; ii) aerosol surface density (S_a); and iii) gas-phase HNO₃ concentration (C_{HNO_3}):

$$R_{\text{HNO}_3} = \frac{dC_{\text{HNO}_3}}{dt} = kC_{\text{HNO}_3} \quad (1)$$

Table 2. Average dust chemical aging indices and maximum HNO₃ uptake rates in East Asia.

Location	Date	$\frac{\overline{[CO_3^{2-}]}}{[Ca^{2+}]+[Mg^{2+}]}$ ¹⁾	$\overline{[NO_3^-]}^{\max}$ ²⁾ ($\mu\text{g}/\text{m}^3$)	$\frac{\Delta\overline{[NO_3^-]}^{\max}}{\Delta t}$ ³⁾ ($\mu\text{g}/\text{m}^3 \cdot \text{hr}$)	Chemical aging time ⁴⁾
Yellow Sea					
ACE-ASIA C130 Flight #6	April 11, 2001	0.87	2.02	0.07	29 hours
ACE-ASIA C130 Flight #7	April 12, 2001	0.68	2.18	0.07	30 hours
Kyushu					
ACE-ASIA C130 Flight #8	April 13, 2001	0.39	1.89	0.05	42 hours
Seoul					
Case I	April 11, 2005	0.87	1.21	0.01	84 hours
Case II	April 15, 2005	0.43	5.65	0.23	25 hours
Case III	April 20, 2005	0.50	5.89	0.26	24 hours

¹⁾Ratio averaged over the flight paths (ACE-ASIA Flights) and over the measured periods (Seoul).

²⁾ $\overline{[NO_3^-]}^{\max} = \overline{[NO_3^-]} + \overline{[SO_4^{2-}]}$

³⁾The average production rate of $\overline{[NO_3^-]}^{\max}$

⁴⁾Estimated elapsed times between pollution plume injections and measurements

$$k = \frac{1}{4} v_{HNO_3} \gamma_{HNO_3} S_a \quad (2)$$

where k denotes the mass transfer coefficient (1/s), v_{HNO_3} the molecular mean velocity of HNO₃ (cm/s), and S_a the aerosol surface density ($\mu\text{m}^2/\text{cm}^3$). In this study, we discuss these three possibly influential factors to determine which factor (or factors) is really responsible for the observed discrepancy in R_{HNO_3} onto dust particles.

2.2 Reaction Probability of HNO₃ (γ_{HNO_3})

First of all, the slow R_{HNO_3} could result from low γ_{HNO_3} onto dust particles. As mentioned in the Introduction, large differences have been reported in the magnitude of γ_{HNO_3} onto dust particles (Song *et al.*, 2007; Johnson *et al.*, 2005; Umann *et al.*, 2005; Harnisch and Crowley, 2001a, b; Underwood *et al.*, 2001a, b; Fenter *et al.*, 1995). Fig. 1 presents how fast HNO₃ can be transferred from the gas phase into dust particles with different γ_{HNO_3} values, using eqns. (1) and (2). For example, when $\gamma_{HNO_3} = 0.1$, the 10 e-folding lifetime (τ_{10} , defined as the time at which $C_{HNO_3}/C_{HNO_3,0} = 1/10e = 0.037$; $\tau_{10} = (1 + \ln 10)/k$, where k represent the mass transfer coefficient in eqn. (2)) is only 1.41 hrs. When $\gamma_{HNO_3} = 0.01$, τ_{10} becomes 8.03 hrs. In other words, 96.3% of HNO₃ is partitioned into the particulate phase within 8.03 hrs, when $\gamma_{HNO_3} = 0.01$. The partitioned HNO₃ is then rapidly converted into nitrate, being associated with Ca²⁺ and Mg²⁺ ions inside the dust particles. For example, if the HNO₃ levels of 1-3 ppb are converted into nitrate at STP at a yield of 96.3%, nitrate concentrations of 2.6-7.7 $\mu\text{g}/\text{m}^3$ should be found in the dust particles after relatively short chemical aging times (within few hours). Once these amounts of nitrate are formed in the dust particles, the particles

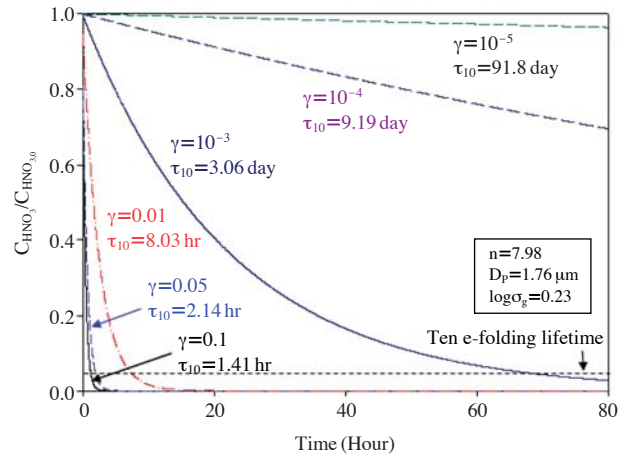


Fig. 1. Ten e-folding lifetimes (τ_{10}) with different reaction probability of HNO₃. The parameters for log-normal aerosol distribution used in this figure are presented in the box (Zhang *et al.*, 1994).

(particularly Ca²⁺) can be completely neutralized only by nitrate in most typical dusty situations. HNO₃ levels of 1-3 ppb were frequently observed with high dust concentrations over the downwind areas from the polluted regions in East Asia (this will be discussed in more detail in section 2.4; also refer to Bauer *et al.* (2004)). However, such large amounts of nitrate have never been found in dust particles, particularly in East Asia (Song *et al.*, 2007; Ro *et al.*, 2005; Song *et al.*, 2005; Zhang *et al.*, 2003). In contrast, when $\gamma_{HNO_3} = 10^{-3}$ - 10^{-5} , R_{HNO_3} become much slower ($\tau_{10} = 3.1$ -91.8 days). With the initial C_{HNO_3} of 1-3 ppb and γ_{HNO_3} of 10^{-4} , the converted amount of nitrate after the interacting times of 8 hours is 0.095-0.29 $\mu\text{g}/\text{m}^3$, which is

equivalent to an hourly averaged R_{HNO_3} of 0.01-0.04 $\mu\text{g}/\text{m}^3 \cdot \text{hr}$. Such slow R_{HNO_3} are more consistent with the slow chemical evolution of dust particles observed in the field measurements. For example, in Table 2, we estimated the possibly maximum nitrate concentrations ($[\text{NO}_3^-]_{\text{max}}$; $[\text{NO}_3^-]_{\text{max}} = [\text{NO}_3^-] + [\text{SO}_4^{2-}]$). The measurement data used in Table 2 were obtained from the ACE-ASIA C130 flight campaign conducted over the Yellow sea on April 11-13, 2001, and a measurement campaign conducted in Seoul in April, 2005. We selected the data from the dust storm periods of the campaigns. In this calculation, while we cannot estimate the individual amounts of nitrate and sulfate, we can estimate the combined amounts of “nitrate+sulfate” concentration in the dust particles by equating the replaced carbonate equivalences to the “nitrate+sulfate” equivalences. In an extreme case, carbonate in dust particles could be replaced only by NO_3^- . These amounts ($[\text{NO}_3^-]_{\text{max}} = [\text{NO}_3^-] + [\text{SO}_4^{2-}]$). are then divided by chemical aging times to obtain the maximum possible nitrate uptake rates. As shown in Table 2, the rates range from 0.01 to 0.26 $\mu\text{g}/\text{m}^3 \cdot \text{hr}$. These values are in general comparable to the estimated rates above (0.01-0.04 $\mu\text{g}/\text{m}^3 \cdot \text{hr}$), particularly for the cases of ACE-ASIA C-130 Flights #6, #7, and #8 which recorded results in the range 0.05-0.07 $\mu\text{g}/\text{m}^3 \cdot \text{hr}$ (again, it is important to remember that the average uptake rates actually represent the production rates of $\text{NO}_3^- + \text{SO}_4^{2-}$).

Although in this study we do not intend to estimate γ_{HNO_3} onto dust particles, one of the objectives of this study is to decide which values of “already-measured” γ_{HNO_3} in Table 1 can be adopted in the dust chemistry modeling studies. Based on the calculations above, the modeling studies with γ_{HNO_3} of $\sim 10^{-3}$ - $\sim 10^{-5}$ could produce more consistent results with the field measurement data.

2.3 Surface Area

There is another possible mechanism that could slow down R_{HNO_3} into dust particles: the application of a

smaller surface area to eqn. (2). For example, in an estimating procedure of γ_{HNO_3} , Umann *et al.* (2005) introduced an “active surface area (S_A)” (for greater detail, refer to both Umann *et al.* (2005) and Matter Engineering, Appendix IV of Operating Instructions LQ1-DC, SKM990318-7b). A similar type of active surface area, so-called “Fuchs surface”, was also introduced by Pandis *et al.* (1991) and Shi *et al.* (2001). Whichever active surface area is used, S_A has a tendency to become smaller than the “geometric surface area” (S_G), when the coarse-mode fraction is large, such as in dust and sea-salt aerosol cases. Therefore, if we use S_A instead of S_G for the gas-to-particle mass transfer process, R_{HNO_3} could become slow. Table 3 presents the typical ratios of S_A to S_G for dust and sea-salt particle distributions (Sander and Crutzen, 1996; Zhang *et al.*, 1994; Jaenicke, 1993). The ratios range between 0.11 and 0.41. In particular the ratio is 0.11 for the two typical dust cases, indicating that R_{HNO_3} become slower by a factor of 0.11, even if the same γ_{HNO_3} is used. Here, the relevant question is whether S_A can be applied to eqn. (2). Umann *et al.* (2005) used S_A with the concept of the “actual surface area” that is accessible for impinging gas molecules that can typically be measured by a BET (Brunauer, Emmett and Teller) type of instrument. However, both the active ($\mu\text{m}^2/\text{cm}^3$) and Fuchs ($1/\text{cm}^3$) surface areas are not the “actual/accessible surface area”, but an imaginary aerosol-surface area conveniently adjusted to consider the changing mechanism in the gas-to-particle mass transfer in accordance with the aerosol size changes (Pandis *et al.*, 1991). For the fine particles, the gas-to-particle mass transfer (uptake) rates are proportional to the second moment (i.e., surface area), whereas for the coarse particles, R_{HNO_3} are proportional to the first moment (i.e., radius). Therefore, the S_A -to- S_G ratios are small when the coarse aerosol fraction is large, whereas the ratios are close to unity when the fine fraction is dominant. The variation in uptake mechanism with the aerosol size can be taken into account by the use of Fuchs and Sutugin kinetics (1971) or other

Table 3. Mass transfer coefficients with different types of surface area ($\gamma_{HNO_3}=0.033$).

Aerosol type and size distribution	S_G ($\mu\text{m}^2/\text{cm}^3$)	S_A ($\mu\text{m}^2/\text{cm}^3$)	S_A/S_G	k_A (1/s)	k_G (1/s)	k_F (1/s)
Dust						
Jaenicke (1993) ¹⁾	149.48	16.65	0.11	4.26×10^{-5}	3.82×10^{-4}	2.63×10^{-4}
Zhang <i>et al.</i> (1994) ²⁾	137.07	15.72	0.11	4.02×10^{-5}	3.50×10^{-4}	3.12×10^{-4}
Sea salt						
Jaenicke (1993)	44.54	18.06	0.41	4.97×10^{-5}	1.36×10^{-4}	1.15×10^{-4}
Sander and Crutzen (1996) ³⁾	71.08	5.15	0.07	1.32×10^{-5}	1.82×10^{-4}	1.45×10^{-4}

¹⁾ The parameters have also appeared in Seinfeld and Pandis (1998) (see p. 430)

²⁾ $n=7.98$; $r_p=0.88 \mu\text{m}$; $\log\sigma_g=0.23$

³⁾ $n=1.40$, $r_p=1.66 \mu\text{m}$; $\log\sigma_g=0.19$

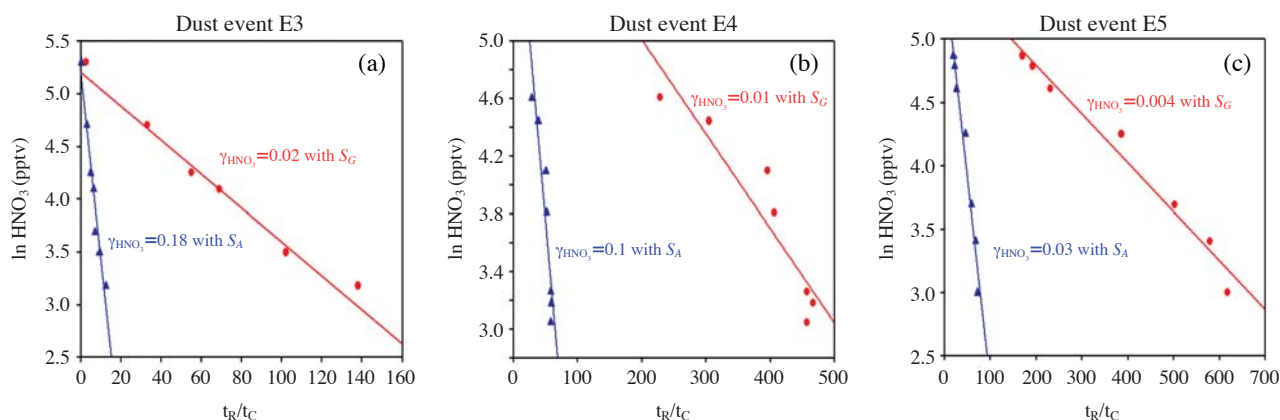


Fig. 2. Estimation of γ_{HNO_3} with two different types of surface areas (S_A and S_G).

similar kinetics (e.g., see p. 604 in Seinfeld and Pandis, 1998). In Table 3, the Fuchs-Sutugin mass transfer coefficient (k_F) is compared with k_A (k from eqn. 2 with S_A for S_a) and k_G (k from eqn. 2 with S_G for S_a). As shown in Table 3, the values of k_G are consistent with k_F , whereas the values of k_A are smaller than k_F by a factor of ~ 0.1 . Meanwhile, the use of S_A in eqn. (2) also leads to an erroneous estimation of γ_{HNO_3} . One example of the erroneous results is shown in Fig. 2. Umann *et al.* (2005) estimated γ_{HNO_3} from the field measurements in Sahara desert, using equations (1) and (2) with S_A . We selected three dust episodes (E3, E4, and E5) from Umann *et al.*'s work (2005), and then re-estimated γ_{HNO_3} with S_A and S_G . As shown in Fig. 2, when S_G is used instead of S_A , the values of γ_{HNO_3} are decreased down to 0.004–0.02, which are smaller than Umann *et al.*'s values ($\gamma_{\text{HNO}_3} = 0.03$ –0.18). These values are also closer to the second group of γ_{HNO_3} in Table 1 that we recommended to be used in the future dust chemistry modeling studies.

2.4 HNO₃ Concentration in the Gas Phase (C_{HNO_3})

The third factor that could affect R_{HNO_3} into dust particles is C_{HNO_3} (from eqn. 1). If C_{HNO_3} is low, R_{HNO_3} becomes slow. Or, if the amounts of HNO₃ are not sufficient, the amounts of nitrate formed in dust particles can be limited by the insufficient the amounts of HNO₃, even with fast R_{HNO_3} . Particularly, extremely low C_{HNO_3} could occur over the areas where NH₃ concentrations are high. Over such areas, HNO₃ can be depleted by the reaction of $\text{HNO}_3(\text{g}) + \text{NH}_3(\text{g}) \rightarrow \text{NH}_4\text{NO}_3(\text{aerosol})$. For example, East Asia has large NH₃ emissions (Kim *et al.*, 2006). Fig. 3 presents C_{HNO_3} and the Ca²⁺ concentrations measured by TRACE-P DC-8 Flights #9 and #13 over the Yellow Sea and East China Sea (see panels (c) and (g)). As presented in pan-

els (d) and (h), the air masses originated from the Gobi desert and the arid areas in Inner Mongolia, and then passed through the highly polluted, high NO_x and NH₃ emission areas in China such as Beijing, Tianjin, Qingdao, Dalian, Nanjing, and Shanghai, as well as various Chinese agricultural areas (Kim *et al.*, 2006). The high levels of Ca²⁺ indicate that the air masses intercepted by DC-8 Flights #9 and #13 contained high levels of dust particles. In the two flights, the observed levels of HNO₃ were increased up to as high as 7 ppb (see panel (g)). The typical HNO₃ levels reported from other TRACE-P DC-8 and P3-B flights in the boundary layer under the continental outflow situations ranged between ~ 1 ppb and ~ 3 ppb. Despite the coexistence of the high levels of dust particles and HNO₃, Song *et al.* (2007; 2005) reported very low nitrate (and/or sulfate) concentrations inside dust particles over the areas close to the flight paths of TRACE-P DC-8 Flights #9 and #13. This is an important correction to the results from Meskhidze *et al.* (2003). They insisted that the coexistence of high levels of Ca²⁺ and HNO₃ in the TRACE-P DC-8 Flight #13 was firm evidence that HNO₃ had already filled up the dust particles (i.e., complete neutralization of Ca²⁺ or 100% carbonate replacement had occurred).

Again, the presence of high HNO₃ levels indicates that the low nitrate concentrations in the dust particles were not a result of the low C_{HNO_3} levels, but were rather due to the small γ_{HNO_3} that was reduced even smaller than 10^{-3} .

3. CONCLUSIONS

The observed R_{HNO_3} onto dust particles were much slower than previously estimated. In addition, R_{HNO_3} have been overestimated in several previous dust

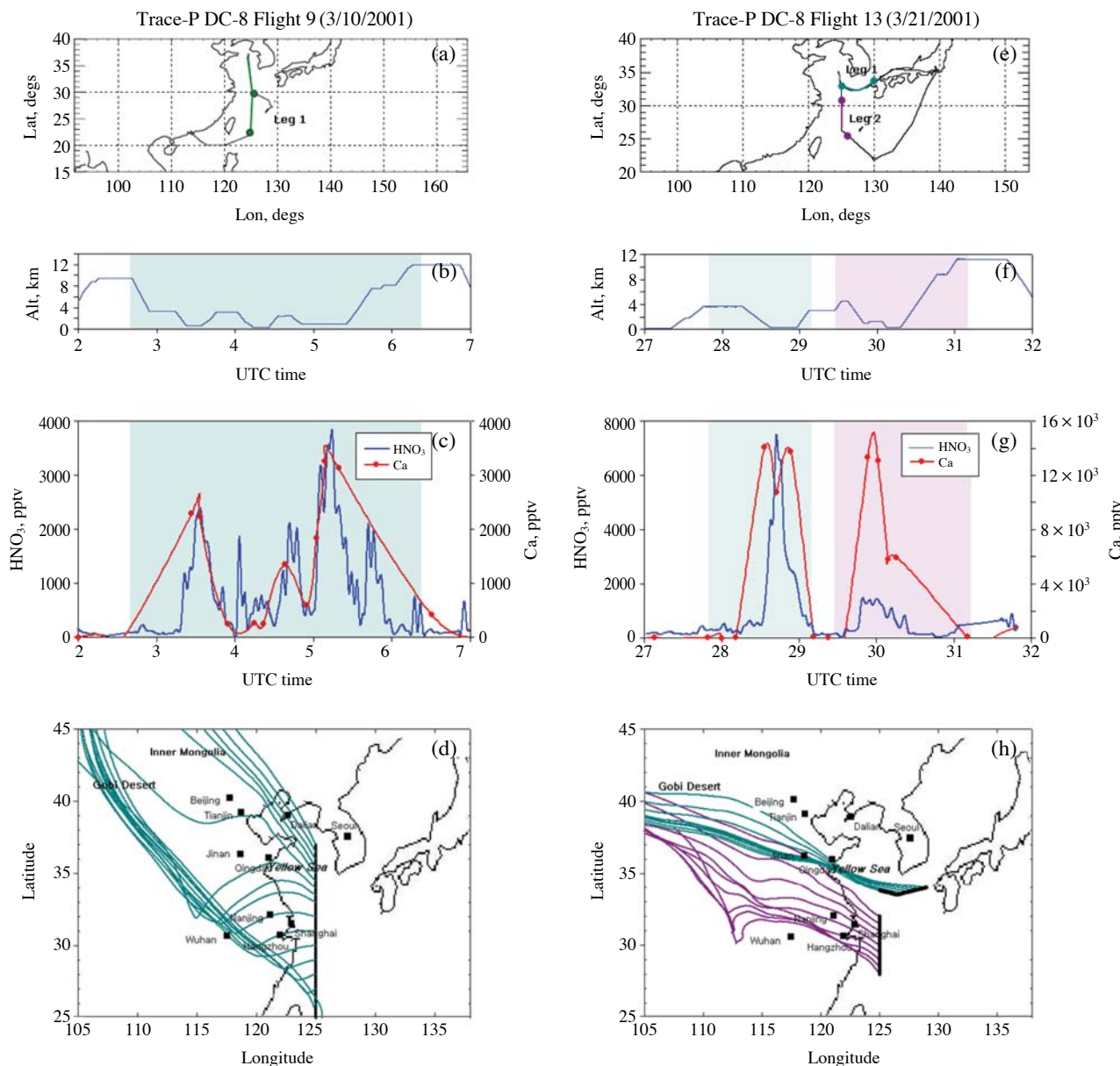


Fig. 3. The HNO₃ and Ca²⁺ concentrations encountered by TRACE-P DC-8 Flights #9 and #13: (a) and (e) flight paths; (b) and (f) altitudes of the flights; (c) and (g) HNO₃ and Ca²⁺ concentrations; and (d) and (h) five-day backward trajectory analyses, respectively, using the HYSPLIT model and meteorological data available on the NOAA/ARL web site (Draxler and Hess, 1998).

modeling studies, for which three possibilities were discussed here: (1) the magnitude of γ_{HNO_3} , (2) aerosol surface area, and (3) C_{HNO_3} . Regarding the second factor, we suggested that S_G should be used in eqn. (2) instead of S_A , which had been used, for example, in Umann *et al.*'s study (2005). With respect to the third factor, we showed that the observed C_{HNO_3} was relatively high, sometimes increasing up to as high as ~ 7 ppb in the marine boundary layer in East Asia, for example. C_{HNO_3} can not limit nitrate formation in dust particles.

The over-predicted R_{HNO_3} onto the dust particles may have been caused by the first factor-overestimated γ_{HNO_3} values ($\gamma_{\text{HNO}_3} = 10^{-1}$ - 10^{-2}). In the previous modeling studies of Dentener *et al.* (1996), Zhang and Carmichael (1999), and Bauer *et al.* (2004), γ_{HNO_3} values of 0.1 and 0.01 were used. In contrast to these overestimated γ_{HNO_3} values, smaller γ_{HNO_3} values within the range 10^{-3} - 10^{-5} have also been reported by Underwood *et al.* (2001a, b) and Johnson *et al.* (2005). In this study we concluded that the use of γ_{HNO_3} values between

$\sim 10^{-3}$ and $\sim 10^{-5}$ could produce more realistic results than those within the range of 10^{-1} - 10^{-2} could, by more accurately predicting the nitrate formation characteristics in dust particles.

ACKNOWLEDGEMENTS

This work was financially supported by the Mid-Career Research Program, through a National Research Foundation of Korea (NRF) grant from the Ministry of Education, Science and Technology (MEST) (2010-0014058); and a National Research Foundation of Korea (NRF) grant funded by the Korea government (MEST) (No. R17-2008-042-01001-0).

REFERENCES

- Bauer, S.E., Balkanski, Y., Schulz, M., Hauglusteine, D. (2004) Global modeling of heterogeneous chemistry on mineral aerosol surfaces: Influence on tropospheric ozone chemistry and comparison to observations. *Journal of Geophysical Research-Atmospheres* 109, D02304, doi:10.1029/2003JD003868.
- Dentener, F.J., Carmichael, G.R., Zhang, Y., Lelieveld, J., Crutzen, P.J. (1996) Role of mineral aerosol as a reactive surface in the global troposphere. *Journal of Geophysical Research-Atmospheres* 101, 22869-22889.
- Draxler, R.R., Hess, G.D. (1998) An overview of the HYSPLIT_4 modeling system for trajectories, dispersion and deposition. *Australian Meteorological Magazine* 47(4), 295-308.
- Fenter, F., Caloz, F., Rossi, M.J. (1995) Experimental evidence for the efficient "Dry deposition" of nitric acid on calcite. *Atmospheric Environment* 29(22), 3365-3327.
- Fuchs, N.A., Sutugin, A.G. (1971) High dispersed aerosols, in *Tropics in Current Aerosol Research* (Hidy, G.M. and Brock, J.R. Eds), Peragamon, New York, pp. 1-200.
- Hanisch, F., Crowley, J.N. (2001a) Heterogeneous reactivity of gaseous nitric on authentic mineral dust samples, and on individual mineral and clay mineral components. *Physical Chemistry Chemical Physics* 3, 2474-2482.
- Hanisch, F., Crowley, J.N. (2001b) Heterogeneous reactivity of gaseous nitric acid on Al₂O₃, CaCO₃, and atmospheric dust samples: A Knudsen cell study. *Journal of Physical Chemistry A* 105, 3096-3106.
- Jaenicke, R. (1993) Troposphere aerosols, in *Aerosol-Cloud-Climate Interactions* (Hobbs, P.V. Ed.), Academic Press, San Diego, pp. 1-31.
- Johnson, E.R., Sciegienka, J., Carlos-Cuellar, S., Grassian, V.H. (2005) Heterogeneous uptake of gaseous nitric acid on dolomite (CaMg(CO₃)₂) and calcite (CaCO₃) particles: A Knudsen cell study using multiple, single, and fractional particle layers. *Journal of Physical Chemistry A* 109, 6901-6911.
- Kim, K.J., Song, C.H., Ghim, Y.S., Won, J.G., Yoon, S.C., Carmichael, G.R., Woo, J.-H. (2006) An investigation on NH₃ emissions and particulate NH₄⁺ and NO₃⁻ formation in East Asia. *Atmospheric Environment* 40, 2139-2150.
- Maxwell-Meier, K., Weber, R.J., Song, C.H., Orsini, D., Ma, Y., Carmichael, G.R., Streets, D.G., Blomquist, B. (2004) Inorganic composition of fine particles in mixed mineral dust-pollution plumes observed from airborne measurements during ACE-Asia. *Journal of Geophysical Research-Atmospheres* 109, D19S07, doi:10.1029/2003JD004464.
- Meskhidze, N., Chameides, W.L., Nenes, A., Chen, G. (2003) Iron mobilization in mineral dust: Can anthropogenic SO₂ emissions affect ocean productivity. *Geophysical Research Letters* 30(21), 2085, doi:10.1029/2003GL018035.
- Pandis, S.N., Baltensperger, U., Wolfenbarger, J.K., Seinfeld, J.H. (1991) Inversion of aerosol data from the epiphaniometer. *Journal of Aerosol Science* 22(4), 417-428.
- Ro, C.-U., Hwang, H., Kim, H., Chun, Y., Van Grieken, R. (2005) Single particle characterization of four "Asian Dust" samples collected in Korea, using low-Z particle electron probe X-ray microanalysis. *Environmental Science & Technology* 39, 1409-1419.
- Sander, R., Crutzen, P.J. (1996) Model study indicating halogen activation and ozone destruction in polluted air masses transported to the sea. *Journal of Geophysical Research-Atmospheres* 101, D4, doi:10.1029/95JD03793.
- Seinfeld, J.H., Pandis, S.N. (1998) *Atmospheric chemistry and physics*. A Wiley-Interscience Publication, New York, p. 604.
- Shi, J.P., Harrison, R.M., Evans, D. (2001) Comparison of ambient particle surface area measurement by epiphaniometer and SMPS/APS. *Atmospheric Environment* 35, 6193-6200.
- Song, C.H., Carmichael, G.R. (2001) Gas-particle partitioning of nitric acid modulated by alkaline aerosol. *Journal of Atmospheric Chemistry* 40, 1-22.
- Song, C.H., Maxwell-Meier, K., Weber, R.J., Kapustin, V., Clarke, A. (2005) Dust composition and mixing state inferred from airborne composition measurements during ACE-Asia C130 Flight#6. *Atmospheric Environment* 39, 359-369.
- Song, C.H., Kim, C.M., Lee, Y.J., Carmichael, G.R., Lee, B.K., Lee, D.S. (2007) An evaluation of reaction probabilities of sulfate and nitrate precursors onto East Asian dust particles. *Journal of Geophysical Research-Atmospheres* 112, D18206, doi:10.1029/2006JD008092.
- Umann, B., Arnold, F., Schaal, C., Hanke, M., Uecker, J., Aufmhoff, H., Balkanski, Y., Van Dingenen, R. (2005) Interaction of mineral dust with gas phase nitric acid and sulfur dioxide during the MINATORIC II field

- campaign: First estimate of the uptake coefficient γ_{HNO_3} from atmospheric data. *Journal of Geophysical Research-Atmospheres* 110, 22306-22323.
- Underwood, G.M., Li, P., Al-Abadleh, H., Grassian, V.H. (2001a) A knudsen cell study of the heterogeneous reactivity of nitric acid on oxide and mineral dust particles. *Journal of Physical Chemistry A* 105, 6609-6620.
- Underwood, G.M., Song, C.H., Phadnis, M., Carmichael, G.R., Grassian, V.H. (2001b) Heterogeneous reactions of NO_2 and HNO_3 on oxides and mineral dust: A combined laboratory and modeling study. *Journal of Geophysical Research-Atmospheres* 106, 18055-18066.
- Zhang, D., Iwasaka, Y. (1999) Nitrate and sulfate in individual Asian dust-storm particles in Beijing, China in the spring of 1995 and 1996. *Atmospheric Environment* 33, 3213-3223.
- Zhang, D., Zang, J., Shi, G., Iwasaka, Y., Matsuki, A., Trochkin, D. (2003) Mixture of individual Asian dust particles at a coastal site of Qingdao, China. *Atmospheric Environment* 37, 3895-3901.
- Zhang, Y., Sunwoo, Y., Kothamarthi, V., Carmichael, G.R. (1994) Photochemical oxidant processes in the presence of dust: An evaluation of the impact of dust on particulate nitrate and ozone formation. *Journal of Applied Meteorology* 33, 813-824.
- Zhang, Y., Carmichael, G.R. (1999) The role of mineral aerosol in tropospheric chemistry in East Asia-A model study. *Journal of Applied Meteorology* 38(3), 353-366.

(Received 4 April 2011, accepted 22 April 2011)